Four-Dimensional Image Reconstruction Strategies in Cardiac-Gated and Respiratory-Gated PET Imaging

Arman Rahmim, PhD[a,*], Jing Tang, PhD[b],
Habib Zaidi, PhD, PD[c,d,e]

KEYWORDS

• PET • Motion tracking • Motion correction • Cardiac gating • Respiratory gating
• 4D image reconstruction • 5D image reconstruction

KEY POINTS

- Cardiac and/or respiratory gating leads to enhanced noise levels, thus producing images with reduced quality.
- Direct four-dimensional (4D) PET image reconstruction incorporating motion compensation provides a very promising alternative to this problem.
- A wide-ranging choice of techniques are available in research settings but have not yet been used in the clinic.
- The development of advanced 4D physical anthropomorphic phantoms and computational models will benefit research in cardiac-gated and respiratory-gated PET imaging.

INTRODUCTION

Positron emission tomography (PET) is a powerful modality for numerous oncologic and cardiac imaging applications. However, when PET is used for chest or upper abdomen examinations, respiratory motion can lead to blurring and distortion of the images. Cardiac imaging applications also suffer from both cardiac and respiratory movements of the heart. Much worthwhile research has focused during the last decade on developing motion compensation techniques to provide more accurate PET images[1,2]; e.g. for the diagnosis and assessment of lung and upper abdomen cancer. It is expected that better PET images will lead to improved detection of small lesions and enhance the ability to assess the extent of the cancer. In some cases, more accurate assessment of chest and upper abdomen lesions may mean that patients can avoid the trauma and expense of surgery. It is expected that physicians will be able to make more informed decisions about how to treat patients with cancer

This work was supported by the Swiss National Science Foundation under grant SNSF 31003A-135576, Geneva Cancer League, the National Science Foundation under grant ECCS 1228091 and the Indo-Swiss Joint Research Programme ISJRP 138866.
[a] Division of Nuclear Medicine, Department of Radiology, Johns Hopkins University, Johns Hopkins Outpatient Centre, Room 3245, 601 N. Caroline Street, Baltimore, MD 21287, USA; [b] Department of Electrical & Computer Engineering, Oakland University, 2200 N Squirrel Road, Rochester, MI 48309, USA; [c] Division of Nuclear Medicine and Molecular Imaging, Geneva University Hospital, Geneva CH-1211, Switzerland; [d] Geneva Neuroscience Center, Geneva University, Geneva CH-1211, Switzerland; [e] Department of Nuclear Medicine and Molecular Imaging, University Medical Center Groningen, University of Groningen, Groningen 9700 RB, Netherlands
* Corresponding author.
E-mail address: arahmim1@jhmi.edu

PET Clin 8 (2013) 51–67
http://dx.doi.org/10.1016/j.cpet.2012.10.005

pet.theclinics.com

lesions in the chest and upper abdomen, particularly when enhanced PET imaging is used in conjunction with structural (CT or MR) scanning. Similarly, in cardiac imaging applications, enhanced clinical tasks will be possible, as elaborated shortly.

A solution to the problem of motion is to perform cardiac and/or respiratory gating of the data, followed by reconstructions of individual gated datasets. However, gating leads to enhanced noise levels and images of reduced quality are generated, which in turn can also lead to enhanced noise-induced bias and variance in kinetic parameters.[1]

An advanced approach to PET imaging is to move beyond pure gating and to obtain enhanced images by making collective use of the gated data sets. Two general schemes may be considered: (1) postreconstruction registration and summation of the independently reconstructed images (eg,[3–7]); (2) incorporation of motion information within the reconstruction algorithm: this latter approach is broadly referred to as four-dimensional (4D) reconstruction, which is the topic reviewed in this article. Asma and colleagues[8] and Chun and Fessler[9] theoretically analyzed and compared postreconstruction versus 4D reconstruction approaches with motion compensation, and showed that noise variance in the latter is less than or comparable with the variance in the former, and the gap between them is larger when less regularization is used[8] and when the gate frames have significantly different counts.[9]

Dynamic imaging and motion-compensated imaging methods overlap in the sense that they both deal with varying activity distributions over time, and 4D methods have been developed for both. The underlying bases of the two are different and need to be distinguished from one another. In particular, some types of motion (and thus certain changes in voxel intensity) are physically/anatomically impossible. 4D image reconstruction algorithms applicable to dynamic imaging have been reviewed elsewhere,[10] whereas here we focus on techniques to model and incorporate motion. Overall, we believe that strategies attempting to apply general 4D PET image reconstruction techniques (such as use of temporal basis functions) to motion compensation (eg, Refs.[11,12]) remain to be further refined or constrained to ensure meaningful reconstructions. Aiming to exploit the periodic nature of cardiac motion, a promising approach[13] was to use temporal Fourier harmonic basis functions to model voxel intensity variation across the gates.

The first section of this article reviews application of 4D image reconstruction methods to cardiac imaging applications, which may involve cardiac or respiratory gating. The next section reviews applications beyond cardiac imaging (particularly, oncology) involving respiratory motion correction only. Some important areas of future research are discussed at the end.

CARDIAC IMAGING APPLICATIONS

Cardiac movements introduce notable visual and quantitative degradations in PET imaging: the base of the heart typically moves 9 to 14 mm toward the apex, and the myocardial walls thicken from approximately 10 mm to more than 15 mm between the end-diastole and end-systole.[14] The motivation behind motion correction in cardiac imaging is two-fold:

i. To further improve the quality of cardiac PET images (noise, resolution) so as to enhance identifiability of radiotracer uptake defects in the left ventricle (LV) by clinicians, because regions of decreased radiotracer uptake can indicate hibernating or infracted myocardial tissue.[15] This finding is also important when applying quantitative measures of perfusion and metabolic parameters in dynamic compartmental modeling studies.[16]
ii. Measurement of motion itself can be useful for characterizing cardiac function.[17] Measures such as ejection fraction and regional wall thickening may be derived from a measure of contractile motion in this way.

We first focus on efforts using cardiac gating only (additional respiratory gating in the context of cardiac imaging is discussed later). Postreconstruction motion correction approaches involving nonrigid registration and summation of individually gated cardiac images have been reviewed elsewhere.[1,2,18]

Cardiac Motion Estimation Methods

Cardiac motion (ie, the contraction of LV during the cardiac cycle) was commonly described by relatively global measures before techniques were developed to estimate the dense motion vector fields (ie, voxel-by-voxel point correspondences). Global parameters such as ejection fraction,[19] longitudinal shortening,[20] radial contraction, and wall thickening[21] provide diagnostic information about the cardiac function. Other than providing a more elaborate description of cardiac motion, a major objective of obtaining the dense motion field is to compensate for motion in cardiac-gated imaging and arrive at reduced blurring artifacts without intensifying noise levels.[22–25]

Compared with emission tomography imaging, tagged MR imaging provides a more favorable environment for calculation of the dense motion field (myocardial tagging involves production of a spatial pattern of saturated magnetization, eg, at end-diastole, and then imaging the resulting deformation of the pattern as the heart contracts through the cardiac cycle).[26–28] The difference in intensities between tagged and untagged regions allows tracking of the motion of underlying tissues. Young and colleagues[29] presented a method for tracking stripe motion in the image plane and showed how the information could be incorporated into a finite-element model of underlying deformation. The method provided a framework to combine high-level global constraints (eg, smoothness and connectivity) with low-level local constraints (eg, dark, linear features). Park and colleagues[30] presented a technique using a class of physics-based deformable models allowing parameterized deformations that captured the motion of the LV. Ozturk and McVeigh[31] used 4D B-splines to interpolate the motion between the tracked myocardial points. The 4D displacement field formed by combining the two-dimensional (2D) fields, as derived from the short-axis and long-axis image planes, could be used to track the deformation of points anywhere within the myocardium. Osman and colleagues[32] proposed a method that estimates cardiac motion applied to spatial modulation of magnetization (SPAMM)-tagged MR images. The SPAMM-tagged images have a collection of distinct spectral peaks in the Fourier domain, each of which contains information about the motion in a certain direction. The inverse Fourier transform of just one of these peaks is a complex image, the phase of which is linearly related to a directional component of the true motion. These investigators defined the harmonic phase (HARP) image to be the principle value of the phase of the complex image and used the HARP image to measure small displacement fields. The main characteristic of this method is its computational simplicity.

We discuss these methods for tagged MR images not only for the completeness of the literature review on cardiac motion estimation but also to resonate with the recent emergence of integrated PET/MR scanners.[33,34] Recent work by Petibon and colleagues[35] applied cardiac wall motion estimated from tagged MR images in PET image reconstruction for simultaneous PET/MR. This preliminary work reported improved perfusion defect detection using a physical phantom.

For other imaging modalities, different extensions of the classic optical flow approach of Horn and Schunck[36] have been commonly applied. The optical flow technique assumes that a moving point in a sequence of images does not change its intensity. The classic approach invokes local Taylor series approximations [using partial derivatives with respect to the spatial and temporal coordinates]. It was first applied directly to 2D cardiac images in Refs.[37,38] Because 2D motion is inadequate to describe cardiac motion vectors, three-dimensional (3D) extension of the algorithm was provided by Song and Leahy[39] and Zhou and colleagues[40] on CT cardiac sequences. Klein and colleagues[3,9] used a nonuniform elastic regularization function inspired from a linear elastic material model.[41] The motion field is regularized by an energy function constraining the source volume as if it were a physical elastic material being deformed by external forces. In several works in which simultaneous gated image reconstruction and motion estimation were performed,[25,30,42] algorithms including similar regularization via the strain energy function were implemented for the purpose of myocardium motion estimation. These works reported improved noise and resolution characteristics in the reconstructed images (**Fig. 1**). In addition, Gravier and colleagues[24] also performed cardiac motion estimation via the optical flow method, which they subsequently incorporated as temporal regularization in 4D image reconstruction, showing improved accuracy of cardiac images without causing any significant cross-frame blurring.

Optical flow techniques assume that a moving point in a sequence of images does not change its intensity. This assumption may be violated in emission tomography because of the limited spatial resolution (and the resulting partial volume effect), particularly as the myocardium expands and becomes thin in the end-diastolic phase. An alternative is to invoke the continuity equation describing conservation of mass (here, intensity), resulting in an additional term relative to classic optical flow (and sometimes referred to as extended optical flow)[39]; such an approach was recently used by Dawood and colleagues[43] for cardiac motion estimation.

Optical flow algorithms are known for the aperture problem wherein there is not enough information in a small area to uniquely determine motion perpendicular to the direction of the local gradient of the image intensity.[44,45] This problem is commonly tackled via introduction of additional constraints. Nonetheless, the true motion cannot be recovered without a priori knowledge of the motion. Klein and colleagues[9] performed qualitative analysis on tracking the cardiac twist in the healthy PET myocardium. The motion field estimated from PET images, cine MR images, and

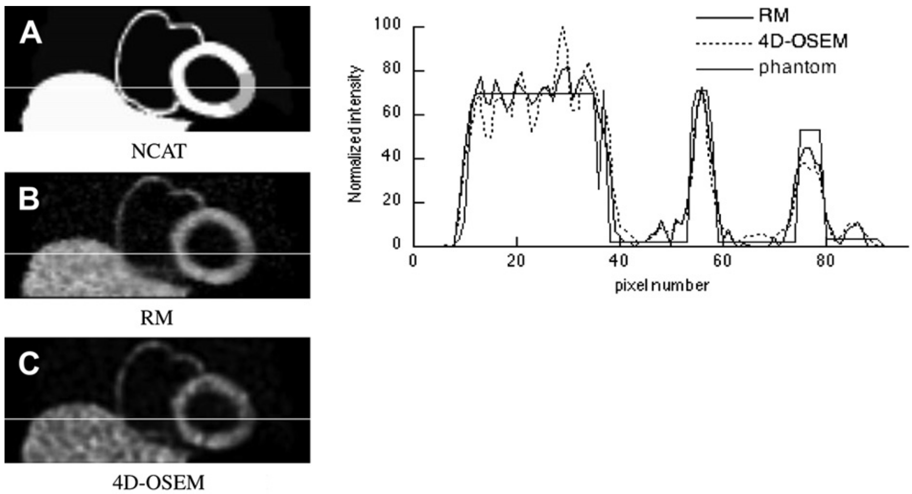

Fig. 1. Sagittal slice of (*A*) the NCAT phantom (truth), (*B*) image reconstructed from the proposed integrated image reconstruction and motion (RM) estimation algorithm, and (*C*) image reconstructed using the conventional OSEM (ordered subset expectation–maximization) algorithm plus 4D postreconstruction filtering. Profiles of the images along the section indicated by the line. (*Reprinted from* Mair BA, Gilland DR, Sun J. Estimation of images and nonrigid deformations in gated emission CT. IEEE Trans Med Imaging 2006;25(9):1140; with permission.)

tagged MR images was compared. The conclusion was that the component of motion normal to the ventricular surfaces could be accurately estimated; however, because of uniformity in the healthy myocardium in PET imaging, the torsion component was considerably more difficult to track. Cine MR images with higher resolution did not augment the ability of the optical flow technique in terms of catching the twist motion. Only tagged MR images had sufficient features for the algorithm to accurately estimate the motion.

The performance of the optical flow technique to estimate cardiac motion from emission tomography images was evaluated quantitatively by Tang and colleagues.[46] Using the 4D NCAT (NURBs (nonuniform rational B-splines) Cardiac Torso) phantom with a known motion vector field, the study confirmed that the optical flow technique could not appropriately estimate tangential motion for uniform myocardial perfusion patterns. It also showed that without detection of the tangential motion, the estimated radial motion also deviates from the truth, because the motion components are correlated with each other.

Besides optical flow methods, some other techniques were investigated for motion-compensated image reconstruction. For example, the motion-frozen technique by Slomka and colleagues,[47] originally applied to single-photon emission CT (SPECT), involved detecting the epicardial and endocardial surfaces and tracking their movements, followed by extrapolation of the movements of the surfaces to other points. The technique was also applied in PET image reconstruction,[8] resulting in significantly enhanced (P<.05) contrast and contrast/noise ratios in fluorodeoxyglucose myocardial viability images.

Reconstruction Methods

In the following sections, four general 4D reconstruction approaches are reviewed: those in which motion estimation is performed (1–3) before or (4) during 4D image reconstruction.

1. Interiterative temporal smoothing: given the estimated motion vectors enabling tracking of any given voxel across the cardiac gates, this approach imposes temporal smoothing across the gated images after every iteration of the reconstruction algorithm. Such an approach was suggested by Brankov and colleagues,[48] who in addition replaced the uniform-voxel framework with mesh modeling within image reconstruction[49] (an efficient image description based on nonuniform sampling; mesh nodes are placed more densely in image regions having finer detail). However, the investigators seem to have abandoned this approach in favor of postreconstruction motion-compensated filtering in later publications.[50,51] Overall, spatial[52,53] or temporal[54,55] interiteration filtering methods are ad hoc (eg, are not proved to be convergent). A more theoretically sound and more popular approach is discussed next.

2. Bayesian maximum a posteriori (MAP) reconstruction: MAP methods[56] attempt to address the ill-posed nature of emission tomography reconstruction via inclusion of spatial or temporal priors.[57] Instead of seeking an image estimate $\vec{f}$ that maximizes the Poisson log-likelihood function $L(\vec{f})$ as is the case with the regular expectation-maximization (EM) algorithm,[58,59] MAP methods seek to maximize the MAP function $L(\vec{f}) - \beta V(\vec{f})$, where $V(\vec{f})$ is a potential function that regularizes the objective function (commonly by penalizing intensity variations within spatial neighborhoods), and β is the MAP hyperparameter to be set by the user for the particular imaging task. A common (although approximate) iterative solution to the MAP formulation can be reached via the one-step-late (OSL) approach of Green,[60] arriving at

$$\vec{f}^{new} = \frac{\vec{f}^{old}}{P^T\vec{1} + \beta \left.\dfrac{\partial V(\vec{f})}{\partial \vec{f}}\right|_{\vec{f}=\vec{f}^{old}}} P^T \frac{\vec{y}}{P\vec{f}^{old}} \quad \textbf{(1)}$$

where $\vec{f}^{old}$ and $\vec{f}^{new}$ denote the previous and updated image estimates, $\vec{y}$ is the projection space data, P is the system matrix modeling the probabilities of detection, and $\vec{1}$ is a column vector with all elements equal to 1.

In addition, Gravier and Yang[61] used a MAP formulation to encourage smoothing across the gated frames, given knowledge of voxel movements from the estimated motion vector field. As an example, denoting the estimated activity for a given gate q (q = 1…Q) as $\vec{f}_q$, the following penalty V_t was considered:

$$V_t = \sum_{q=1}^{Q}\sum_{j=1}^{J}\left[[\vec{f}_q]_j - \frac{1}{Q-1}\sum_{\substack{p=1\\ p\neq q}}^{Q}[M_{p\to q}\vec{f}_p]_j\right]^2 \quad \textbf{(2)}$$

where the subscript j denotes the particular voxel (j = 1…J) in the image, and $M_{p\to q}$ denotes the estimated motion matrix transforming a given image $\vec{f}_q$ to its corresponding distribution in gate p given the estimate motion vectors. The investigators introduced a generalized weighted formulation[24,62] to this expression to weight intergate variations in voxel intensities depending on gate separation (higher weights for nearer gates).

A similar approach was taken by Lalush and colleagues[63,64] but the motion was assumed to be known a priori. However, they obtained similar results when no motion information was considered (ie, $M_{p\to q}$ was set to the identity matrix). This result may have been caused by the limited resolution of their scanner, but has been pursued similarly in several subsequent works.[65–68]

3. The MAP-OSL algorithm (1) of Green[60] is based on an approximation (and breaks down for large values of β). In addition, it is a nontrivial task to select the parameters associated with the prior/penalty term (which play an important role in the image quality) and this is often achieved through trial-and-error. These methods treat the same moving object as different temporal reconstructions that are merely temporally correlated. Nevertheless, a more concrete approach would involve a truly 4D approach, in which the estimated deformations are incorporated within a unified cost function to be optimized (for a single object). Such an approach was proposed and investigated by Qiao and colleagues,[69] Li and colleagues,[70] and Lamare and colleagues,[71] although originally for respiratory gating applications but later also used for cardiac gating.[72] In this approach, the measured nonrigid motion (estimated from the gated images) is modeled in the image-space component of the system matrix of the EM algorithm, and a truly 4D EM reconstruction algorithm has been achieved. This approach is promising because of its accurate and comprehensive modeling of the relation of a moving object to detected events. Introducing a time/gate-varying system matrix P, including decomposition[73–75] into the geometric component G, diagonal normalization N and attenuation A matrices, as well as $M_{1\to q}$ modeling the motion transformation from the reference gate 1 to existing frame q ($P=NAGM_{1\to q}$), one arrives at the 4D EM update algorithm to estimate the image at the reference gate:

$$\vec{f}^{new} = \frac{\vec{f}^{old}}{\vec{s}}\sum_{q=1}^{Q} M_{1\to q}^T G^T \frac{\vec{Y}_q}{GM_{1\to q}\vec{f}^{old}} \quad \textbf{(3)}$$

where the sensitivity image $\vec{s}$ is given by

$$\vec{s} = \sum_{q=1}^{Q} M_{1\to q}^T G^T A^T N^T \vec{1} \quad \textbf{(4)}$$

This approach is analogous to motion-corrected EM reconstructions in brain imaging that move beyond purely correcting[76–78] individual events for motion and that result in modified sensitivity images to account for the impact of motion on probabilities of detection.[79–83]

4. Commonly in the literature, cardiac motion is estimated after reconstruction of individual gated frames; and in the techniques outlined earlier, the extracted motion information is used in subsequent 4D reconstructions to yield enhanced images. However, Gilland and colleagues[22,23,42] hypothesized that, given the close link between the image reconstruction and motion estimation steps, a simultaneous method of estimating the two is better able to (1) reduce motion blur and compensate for poor signal-to-noise (SNR) ratios and to (2) improve the accuracy of the estimated motion. Their proposed algorithm worked by 2-step minimization of a joint energy functional term (which included both image likelihood and motion-matching terms). This work was also extended from a 2-frame approach to the complete cardiac cycle by Gilland and colleagues.[84]

   The approach taken by Jacobson and Fessler[85,86] considered a parametric Poisson model for gated PET measurements involving the activity distribution as unknown as well as a set of deformation parameters describing the motion of the image throughout the scan (from gate to gate). By maximizing the log-likelihood for this model, a technique referred to as joint estimation with deformation modeling was used to determine both the image and deformation parameter estimates jointly from the full set of measured data. A similar motion-aware likelihood function was used by Blume and colleagues,[87] although using a distinct optimization scheme and depicting more convincing results, which is shown in **Fig. 2**. By comparison, the techniques described earlier estimate a single image and N − 1 deformations, whereas the method of Gilland and colleagues estimates N images and N − 1 motion deformations, thus involving a larger number of unknowns; the cost function it uses does not involve deformations in the log-likelihood term, thus potentially simplifying the optimization task. The aforementioned trade-off remains to be elaborately studied.

Dual-Gated Imaging

Respiratory motion of the heart is comparable with myocardial wall thickness[88] and introduces considerable degradations in quantitative accuracy of images[89] and quality of polar maps.[90] Increasingly more attention has been paid to dual gating of the heart in human and animal studies.[88,91–100] Different hardware gating devices developed in academic and corporate settings were exploited to achieve this goal and are described in the article by Bettinardi and colleagues elsewhere in this issue.

Rigid Versus Nonrigid Modeling of the Respiratory Motion of the Heart

Respiratory motion of the heart has been modeled as rigid within several PET[89,101] and SPECT[102] reconstructions. There exists some evidence to this end: analysis[103] of 20 sets of 4D respiratory-gated

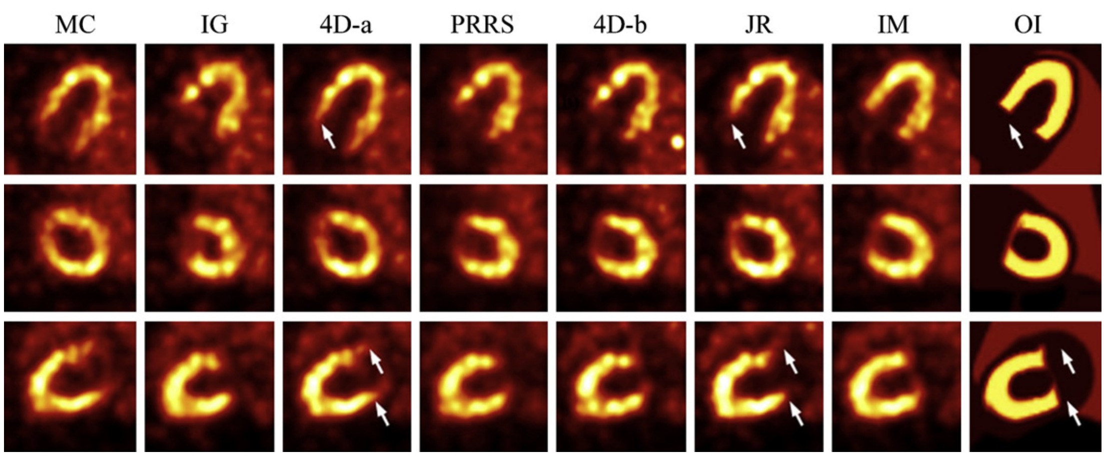

Fig. 2. Selected transverse, coronal, and sagittal slices for different reconstruction scenarios for simulated data (*from left to right*): ML-EM reconstruction of motion-contaminated data (MC), ML-EM reconstruction of the individual gates (IG), 4D method (when motion is estimated from preliminary reconstructions) (*4D-a*), postreconstruction registration and summation (PRRS), 4D method when different gridding is used to estimate motion (*4D-b)*, proposed joint reconstruction (JR), and a motion compensating reconstruction based on the ideal motion (IM). For comparison, the original image (OI) is shown in the last column. (*Reprinted from* Blume M, Martinez-Moller A, Keil A, et al. Joint reconstruction of image and motion in gated positron emission tomography. IEEE Trans Med Imaging 2010;29(11):1896; with permission.)

image data from normal and abnormal humans revealed respiratory motion of the heart (as well as liver, stomach, spleen, and kidneys) to involve for the most part rigid translations downward and to the interior as the diaphragm contracts during inspiration. Furthermore, MR scans performed on 15 normal individuals depicted predominantly translational nature of respiratory-induced movements in upper abdominal organs.[104]

Nonetheless, respiratory motion does induce some nonrigid movements in the heart, as it is pushed and pulled by the diaphragm and other connected tissue: for instance, gated CT studies on dogs[105] recorded an average change of 12% in the total end-diastolic heart volume during forced positive pressure inspiration at 15 cm H_2O. Using echocardiography, similar shape changes were found in human individuals.[106] Furthermore, Klein and colleagues[99] performed quantitative measures of respiratory motion of the heart as extracted from 10 respiratory-gated PET studies. Translations between end-inspiration and end-expiration were often greater than 10 mm and ranged from 1 to more than 20 mm (rigid motion). Moreover, the LV showed nonnegligible compression factors. The LV was generally largest at end-inspiration and smallest at end-expiration. Nonrigid motion was close to 10% in several cases, computed as the product of the 3 extension factors along the x, y, and z directions.

The extension factors were largest along the superior/inferior axis (~5%), which, given the typical 80-mm to 100-mm dimension of the LV along this direction, would result in a heart image that would be 4 to 5 mm too small if motion was assumed simply rigid. Compared with the average 10-mm thickness of the left ventricular wall, this scaling error may therefore be considerable. However, with the ECAT EXACT HR scanner (CTI/Siemens, Knoxville, TN), only small improvements were observed[99] after performing nonrigid motion modeling. It may be concluded that appropriateness of modeling respiratory motion of the heart as rigid versus nonrigid depends on the resolution of the PET scanner. With wider acceptance of reconstruction algorithms incorporating resolution modeling (also referred to as point-spread-function (PSF) modeling),[107–113] and the resulting resolution improvements down to the 2-mm to 3-mm range in clinical scanners, it is expected that nonrigid modeling approaches would serve as more reliable and accurate models of respiratory motion of the heart. Efforts to this end include: (1) use of affine motion models (strictly speaking, an affine model is nonrigid, but in the literature, often it is a class of its own (ie, rigid vs affine vs nonrigid models): this model extends the rigid motion model (6 parameters of rotation and translation) to also allow 3 scale[71] and 3 skew parameters[99] and (2) use of nonrigid B-spline models.[91]

Reconstruction Methods

Modeling respiratory motion of the heart as rigid, Livieratos and colleagues[101] transformed individual lines of response (LORs) (ie, via translations and rotations) to compensate for respiratory motion, followed by standard reconstructions of individual cardiac-gated datasets. Nonetheless, this approach, although appropriately compensating for normalization given original LOR coordinates, did not compensate for duration of time each LOR spends outside the field-of-view because of motion, which can be compensated via multiplication factors applied to the motion-compensated events[114] or modifying the sensitivity images through the 4D EM formalism of Eqs. 3 and 4. Invoking the latter approach, Rahmim and colleagues[89] and Chen and colleagues[91] performed 4D respiratory motion compensation for each cardiac phase. A simulated example from Ref.[89] is shown in **Fig. 3**, wherein short-axis reconstructed images, for a given cardiac gate, show noisy reconstructions with additional respiratory gating (left), blurred images with no respiratory gating (middle), and improved definition with favorable noise using 4D reconstruction approach. Receiver operating characteristic analysis involving numerical channelized Hotelling observer studies revealed significant improvements ($P<.0001$) for the task of perfusion defect detection using 4D EM respiratory motion compensation.

It is possible to pursue 4D reconstruction methods that incorporate both cardiac and respiratory gating information, as pursued by Blume and colleagues,[87] within a comprehensive dual-gated framework using 24 total gates. Nonetheless, in practice, the common approach has been to use 4D reconstruction methods to compensate for respiratory motion within each cardiac gate, followed by postreconstruction registration and summing of cardiac-gated images.[91,115]

Five-Dimensional Motion-Corrected Image Reconstruction

Dynamic imaging of the heart enables quantification of tracer uptake, providing valuable information about heart function, including the abilities to quantify myocardial blood flow and coronary flow reserve,[116,117] thus providing several powerful applications.[118–124] Nonetheless, this modality has remained primarily limited to research, and

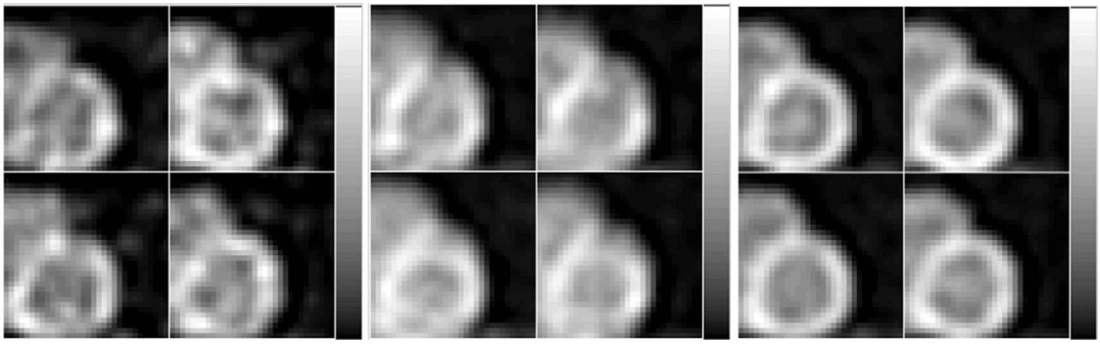

Fig. 3. Short-axis reconstructed images of simulated Rb-82 myocardial perfusion data with 4 noise realizations shown in each set, for the end-diastolic cardiac gate using: *(left)* end-expiration respiratory gate 1, *(middle)* respiratory-nongated data, and *(right)* data processed using 4D EM reconstructions.

remains to be widely adopted in clinical practice; this has been especially related to amplified noise levels caused by subdivision of the data into shorter frames. Novel 4D reconstruction algorithms, aiming to enhance quality and quantitative accuracy of dynamic images, constitute a highly active front and have been reviewed elsewhere.[10,125] Here we discuss some works that have attempted to merge the extra dimensions of cardiac gating and tracer redistribution.

An approach was to use the list-mode capability to first reconstruct the data as gated but static to estimate cardiac motion, followed by application of 4D reconstruction to gated datasets for each dynamic frame.[72] An alternative was to perform 4D image reconstruction to dynamic datasets for each given cardiac gate, followed by postreconstruction filtering across the cardiac gates.[126,127]

By contrast, Jin and colleagues[128] and Gravier and colleagues[62] pursued variations of a more sophisticated five-dimensional (5D) approach of incorporating both dimensions within the reconstruction: they performed preliminary reconstructions to extract the motion vector field; the motion information was then incorporated within objective functions that included weighted variants of (2) penalizing intercardiac-gate intensity variations, although further generalized to also include penalization amongst the dynamic frames. The resulting objective functions were then solved using gradient descent methods. These methods were further refined in Ref.[129] to include a convergent yet fast (ordered subset) reconstruction algorithm framework. Alternatively, Niu and colleagues[130] pursued direct reconstruction of parametric images (from projection data) and incorporated estimated motion vectors within a weighted variant of penalty expression (Eq. 2).

Verhaeghe and colleagues[12] used B-spline temporal basis functions to represent both the temporal and gate dimensions within 5D EM formulation, resulting in improved noise properties and maintaining sharply defined images (however, see note of caution in introduction regarding treatment of motion in the same sense as dynamic tracer evolution).

A different approach to this problem by Shi and Karl[131,132] involved level set methods wherein a variational framework was developed that collectively incorporated region boundaries (assumed to evolve because of motion) and intensities within them. A coordinate descent algorithm was used alternately minimizing the overall energy function with respect to the boundaries and the intensity values. A downside of this approach is that the intensity is assumed to be constant within the defined regions, although additive noise models were included.

Impact of Mismatched AC

When respiratory gating is not used (ie, emission images are contaminated by respiratory motion), the use of high-speed CT images that capture one phase in the respiratory cycle can lead to AC mismatch, visible artifacts, and notable quantitative degradations.[133,134] Potential solutions to this situation include cine CT, CT mapping (using estimated PET motion vectors, 4D-CT acquisition), and many other approaches. This issue is covered in detail in the article by Pan and Zaidi elsewhere in this issue.

With respiratory gating, as also used in 4D reconstruction methods, application of (1) mismatched or (2) averaged/cine CT for AC can also lead to quantitative degradations,[135] and so forth. Therefore, phase-matching methods seem to be the methods of choice.[136] Unlike respiratory motion, cardiac motion is less important in terms of mismatch between emission and transmission images for AC because the heart sac does not really move with cardiac beating.

BEYOND THE HEART: OTHER IMAGING APPLICATIONS INVOLVING RESPIRATORY MOTION CORRECTION

The 4D methods mentioned in the previous section (for cardiac motion correction) are also applicable to 4D respiratory motion correction. Respiratory motion estimation tasks for different organs are discussed first, as incorporated within 4D reconstruction methods.

Respiratory Motion Estimation Methods

Respiratory motion has been modeled as rigid,[102] affine,[99,137] and nonrigid.[43,138–140] Rigid motion and affine deformation modeling were primarily used in conjunction with event rebinning for the correction of respiratory motion.[71] To rebin the PET data by aligning the LOR of each event to the reference position, the motion can be modeled only as rigid or affine because mapping of an LOR is independent of the event location. Modeling respiratory motion as nonrigid thus requires other motion correction techniques, including incorporating the correction in the image reconstruction process[141] and after reconstruction.[142]

When motion is treated as rigid, it has been quantified by tracking translations of some center of mass along the axial direction[102,143] or in 3D.[144] By contrast, the affine deformation model can be solved using image registration techniques to minimize the least squares difference[99] or mutual information.[137] Nonrigid motion estimation is usually treated as a minimization problem with the cost function consisting of (1) a similarity measure between the image frames and (2) a regularization term on the estimated deformation field. Algorithms differ in the measurement of the image similarity and the selection of the regularization. In the following sections, several representative nonrigid motion estimation algorithms are discussed.

Dawood and colleagues[142] proposed an optical flow-based approach in the process of postreconstruction summation of aligned respiratory gates. The method assumed small motion (for the Taylor expansion) and a locally constant flow (as a means to regularize the problem) per the algorithm developed by Lucas and Kanade (LK).[145] The motion needed to be calculated between adjacent gates (to ensure small motion) rather than between the target gate and successive gates. The LK algorithm is comparatively robust in the presence of noise. However, the flow information fades out quickly across motion boundaries. Dawood and colleagues[43] later advanced the local optical flow algorithm by combining it with a global optical flow algorithm (ie, the method of Horn and Schunck [HS]).[36] The HS algorithm uses the smoothness in flow as the constraint and fills in the missing flow information in inner parts of homogeneous objects from the motion boundaries. The respiratory motion was shown to be reduced in the motion-corrected gated images with the correlation coefficient as the criteria. The combined local and global optical flow algorithm was shown to perform better than the local algorithm.

In the method proposed by Ue and colleagues,[140] the deformation field was defined to consist of control points given as the intersection points of grid lines. By moving each control point, the floating image was deformed. The movement at an arbitrary location in the deformation field was calculated by trilinear interpolation of neighbor control points. In their method, the similarity measure between the reference images and the deformed image was based on the principle that the total activity remains the same after the deformation. An expansion ratio, computed by volumes of tetrahedral, was applied on the deformed image to eliminate the discrepancy between the deformed result and the principle. A smoothness constraint in the deformation served as regularization in the objective function, which was minimized using the simulated annealing algorithm.

Bai and Brady[138,139] proposed B-spline deformable registration algorithms in respiratory motion correction of gated PET images. The control point lattice was assumed as a Markov random field (MRF) to regularize the deformation field. B-splines have the advantage of being smooth functions with explicit derivatives and finite support. Both the gated images and the transformation between them were interpolated using cubic B-spline functions. The MRF was assumed to follow the Gibbs distribution based on the Hammersley-Clifford theorem.[146] Gradient descent was used to minimize the cost function, consisting of the mean squared difference between one image and another deformed image and the regularization term.

Reconstruction Methods

Respiratory motion-compensated image reconstruction methods can be grouped into several categories. One category of methods rebins the PET data by aligning the LORs of each event to the reference position using the estimated motion. Because the event-rebinning method mapping of an LOR is independent of the event location, only rigid or affine motion can be incorporated in the process, which can be a viable approach when focusing on specific tumors or organs.[71] Such an approach was originally developed in brain imaging applications (e.g. Ref.[78]).

A considerably more popular category of methods incorporates the estimated motion within the system matrix for image reconstruction. Nonrigid motion can be applied within the reconstruction process. These techniques use a time/gate-varying system matrix and integrate PET projection data acquired at different time bins into a single comprehensive objective function. The 4D EM formulation (3–4) by Qiao and colleagues,[69] Li and colleagues,[70] and Lamare and colleagues,[71] as discussed in the context of Eq. 3, were originally developed for respiratory motion correction. On advent of simultaneous PET/MR imaging, the recent work by Guerin and colleagues[147] used respiratory motion estimated from tagged MR images to reduce motion blur in whole-body PET studies of torso. This motion correction technique and more recent work by the same group[148] fall into this category as well. The time/gate-varying system matrix method was generalized by Qiao and colleagues[149] to incorporate motions only within a user-defined region of interest. In particular, Li and colleagues[70] considered both a phantom experiment and a clinical study with a pancreatic tumor. They showed increased SNR in images reconstructed with the motion-compensated 4D PET reconstruction over that in images from both regular nongated reconstruction and purely gated reconstruction. The motion artifacts were also clearly reduced in the 4D reconstructed images. **Fig. 4** shows reconstructions obtained using (1) nongated PET, (2) conventional purely gated PET, and (3) the 4D EM algorithm using the entire dataset. The SNR ratios were 2.21, 1.83, and 4.17 for the three approaches.

Reyes and colleagues[150] pursued an approach applicable to nongated datasets. A respiratory motion model constructed from MR images was adapted to each patient's anatomy through affine registrations. The resulting estimated motion was then incorporated into the system matrix of the EM algorithm. Compared with the second category methods, this approach does not require motion estimated beforehand or gating. Nevertheless, the robustness of the model-based motion estimation method given the presence of irregular respiratory patterns as well as interpatient respiratory variations remains questionable. Furthermore, analogous investigations in brain imaging (ie, modeling motion contamination within the system matrix without correction of events)[151] have shown suboptimal convergence properties.

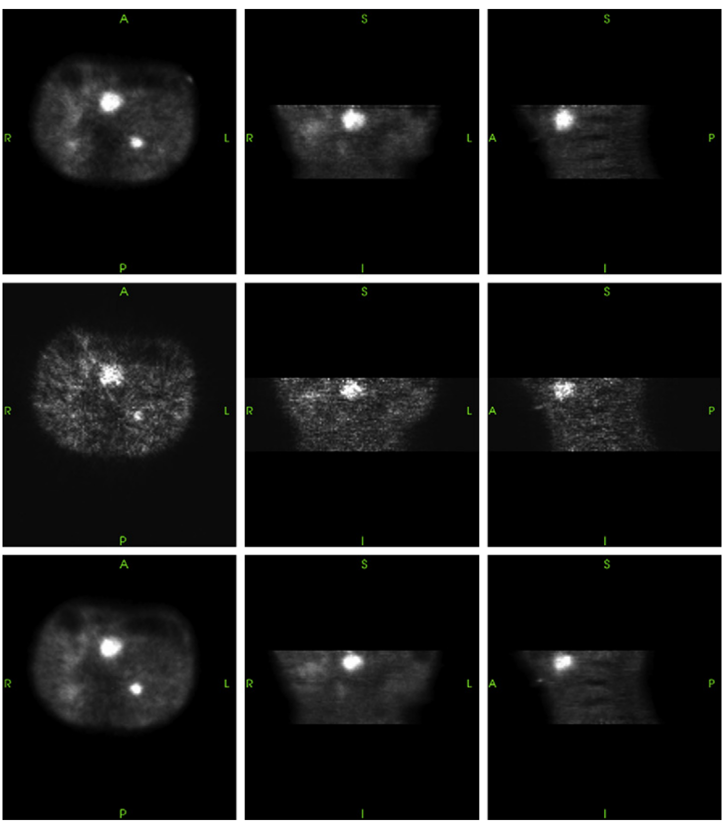

Fig. 4. Reconstructed images of 3D ungated PET obtained by summing all the acquired 4D-PET projections (*top*), conventional 4D PET (*middle*), and model-based 4D PET reconstruction for a clinical study with pancreatic tumor. (*Reprinted from* Li T, Thorndyke B, Schreibmann E, et al. Model-based image reconstruction for four-dimensional PET. Med Phys 2006;33(5):1296; with permission.)

AREAS OF FUTURE RESEARCH

In this section, some areas of research in motion correction are outlined that remain open questions, demanding further inquiries and research:

a. Although theoretic comparisons have been made between postreconstruction and 4D reconstruction methods in which motion is preestimated,[8,9] it remains an open task to theoretically analyze methods in which cardiac or respiratory motion are estimated before or simultaneously with the image reconstruction task. Such analysis might provide insights into further optimization of both categories mentioned earlier, because experimental comparisons have not shown[30,37,42,85,86] a clear advantage of one approach over the other. Development and validation of optimum regularizers, given the distinct spatial resolution properties of motion correction algorithms,[22] is also an area of interest.
b. In dual-gating applications, cardiac versus respiratory gates are commonly treated differently in 4D motion-corrected cardiac imaging applications, wherein the latter are more commonly incorporated within 4D methods, with the former registered and summed after reconstruction.[91,115] However, it is plausible to imagine a combined overall sequence of gates incorporated within the 4D reconstruction framework.[37] Comparison between these two schemes remains an area of interest.
c. Validation and assessment in clinical setting of algorithmic developments in medical imaging is inherently difficult and sometimes unconvincing, particularly when applied to clinical data in the absence of a gold standard, although some approaches to circumvent this limitation have been suggested.[152–154] There is a clear need for guidelines to evaluate image reconstruction and processing techniques in medical imaging research. Task-based assessment of image quality is an emerging field, which will likely help address some of these issues.
d. One of the most active areas of research and development in medical imaging has been the advanced physical anthropomorphic phantoms and computational models that represent the human anatomy[155] and their integration in advanced 4D simulation of time-dependent geometries.[156] Incorporation of accurate models of cardiac and respiratory physiology into the current 4D extended Cardiac-Torso (XCAT) model was a significant step forward to account for inherent cardiac and respiratory motion not considered in the previous models.[157] Besides providing realistic and flexible simulation of normal cardiac motion, Veress and colleagues[158,159] investigated incorporation of a finite-element mechanical model of the LV to accurately model motion abnormalities such as myocardial ischemia and infarction. Besides simulating cardiac motion in the phantom, this model may be applied as a prior in cardiac motion estimation from emission tomography images to recover the true cardiac motion with twist rather than the apparent motion such as that estimated by optical flow methods.[9]

   Likewise, many physical static anthropomorphic phantoms were developed in corporate settings but few dynamic torso phantoms are commercially available and all of them were specifically designed for the assessment of cardiac scanning protocols and ejection fraction calculation software (eg, the dynamic cardiac phantom available from Data Spectrum, Hillsborough, NC). Many academic investigators built dynamic physical phantoms that meet their research needs in cardiac imaging.[160–162] However, similar to commercial systems referred to earlier, virtually none of them incorporate respiratory motion modeling. More advanced technologies allow the construction of dynamic phantoms, allowing modeling of respiratory motion.[163] One interesting design is the platform developed by Fitzpatrick and colleagues,[164] which is capable of programmable irregular longitudinal motion (either artificially generated on a spreadsheet or extracted from respiratory monitoring files) to simulate intrafractional respiratory motion.

SUMMARY

This article summarizes important themes in the emerging field of 4D PET imaging, as applied to cardiac and/or respiratory motion compensation. A wide-ranging choice of techniques are available in research settings but have not yet been used in the clinic. In advanced cardiac and respiratory motion correction schemes, this review has witnessed a general trend to move beyond the noisy images achieved by cardiac-gated and respiratory-gated data which are individually reconstructed, and instead, advanced techniques are seen to make use of novel motion estimation and image reconstruction applications to improve image quality with higher SNR and spatial resolution. There seems to be a general trend toward the use of increasingly sophisticated software for 4D reconstruction in cardiac-gated and

respiratory-gated PET imaging. Strategies that endeavor to apply direct 4D PET image reconstruction techniques to motion compensation seem promising but remain to be further refined or constrained to guarantee meaningful reconstructions.

REFERENCES

1. Nehmeh SA, Erdi YE. Respiratory motion in positron emission tomography/computed tomography: a review. Semin Nucl Med 2008;38(3):167–76.
2. Rahmim A, Rousset OG, Zaidi H. Strategies for motion tracking and correction in PET. PET Clin 2007;2:251–66.
3. Klein GJ, Huesman RH. Four-dimensional processing of deformable cardiac PET data. Med Image Anal 2002;6(1):29–46.
4. Dawood M, Buther F, Lang N, et al. Transforming static CT in gated PET/CT studies to multiple respiratory phases. 18th International Conference on Pattern Recognition. Hong Kong, August 20-24, 2006. p. 1026–9.
5. Schafers KP, Dawood M, Lang N, et al. Motion correction in PET/CT. Nuklearmedizin 2005; 44(Suppl 1):S46–50.
6. Thorndyke B, Schreibmann E, Koong A, et al. Reducing respiratory motion artifacts in positron emission tomography through retrospective stacking. Med Phys 2006;33(7):2632–41.
7. Le Meunier L, Slomka PJ, Dey D, et al. Motion frozen F-18-FDG cardiac PET. J Nucl Cardiol 2011;18(2):259–66.
8. Asma E, Manjeshwar R, Thielemans K. Theoretical comparison of motion correction techniques for PET image reconstruction. IEEE Nuclear Science Symposium Conference Record; San Diego, CA, 29 October - 4 November, 2006. p. 1762–7.
9. Chun SY, Fessler JY. Noise properties of motion-compensated tomographic image reconstruction methods. IEEE Trans Med Imaging in press.
10. Rahmim A, Tang J, Zaidi H. Four-dimensional (4D) image reconstruction strategies in dynamic PET: beyond conventional independent frame reconstruction. Med Phys 2009;36(8):3654–70.
11. Grotus N, Reader AJ, Stute S, et al. Fully 4D list-mode reconstruction applied to respiratory-gated PET scans. Phys Med Biol 2009;54(6): 1705–21.
12. Verhaeghe J, D'Asseler Y, Staelens S, et al. Reconstruction for gated dynamic cardiac PET imaging using a tensor product spline basis. IEEE Trans Nucl Sci 2007;54(1):80–91.
13. Niu XF, Yang YY, Wernick MN. 4D reconstruction of cardiac images using temporal Fourier basis functions. Presented at 15th IEEE International Conference on Image Processing. vols. 1–5. San Diego, CA, October 12-15, 2008. p. 2944–7.
14. O'Dell WG, Moore CC, Hunter WC, et al. Three-dimensional myocardial deformations: calculation with displacement field fitting to tagged MR images. Radiology 1995;195(3):829–35.
15. Di Carli MF, Dorbala S, Meserve J, et al. Clinical myocardial perfusion PET/CT. J Nucl Med 2007; 48(5):783–93.
16. Hutchins GD, Caraher JM, Raylman RR. A region of interest strategy for minimizing resolution distortions in quantitative myocardial PET studies. J Nucl Med 1992;33(6):1243–50.
17. Nichols K, Lefkowitz D, Faber T, et al. Echocardiographic validation of gated SPECT ventricular function measurements. J Nucl Med 2000;41(8): 1308–14.
18. Visvikis D, Lamare F, Bruyant P, et al. Correction de mouvement respiratoire en TEP/TDM. Med Nucl 2007;31(4):153–9 [in French].
19. Pombo JF, Troy BL, Russell RO Jr. Left ventricular volumes and ejection fraction by echocardiography. Circulation 1971;43(4):480–90.
20. Dumesnil JG, Shoucri RM, Laurenceau JL, et al. A mathematical model of the dynamic geometry of the intact left ventricle and its application to clinical data. Circulation 1979;59(5):1024–34.
21. Holman ER, Buller VG, de Roos A, et al. Detection and quantification of dysfunctional myocardium by magnetic resonance imaging. A new three-dimensional method for quantitative wall-thickening analysis. Circulation 1997;95(4):924–31.
22. Cao Z, Gilland D, Mair B, et al. Simultaneous reconstruction and 3D motion estimation for gated myocardial emission CT using the 4D NCAT phantom [abstract]. J Nucl Med 2003; 44(5):9P.
23. Gilland DR, Mair BA, Bowsher JE, et al. Simultaneous reconstruction and motion estimation for gated cardiac ECT. IEEE Trans Nucl Sci 2002; 49(5):2344–9.
24. Gravier E, Yang Y, King MA, et al. Fully 4D motion-compensated reconstruction of cardiac SPECT images. Phys Med Biol 2006;51(18):4603–19.
25. Mair BA, Gilland DR, Sun J. Estimation of images and nonrigid deformations in gated emission CT. IEEE Trans Med Imaging 2006;25(9): 1130–44.
26. Zerhouni EA, Parish DM, Rogers WJ, Yang A, Shapiro EP. Human heart: tagging with MR imaging-a method for noninvasive assessment of myocardial motion. Radiology 1988;169(1): 59–63.
27. Axel L, Dougherty L. MR imaging of motion with spatial modulation of magnetization. Radiology 1989;171(3):841–5.
28. Axel L, Montillo A, Kim D. Tagged magnetic resonance imaging of the heart: a survey. Med Image Anal 2005;9(4):376–93.

29. Young AA, Kraitchman DL, Dougherty L, et al. Tracking and finite-element analysis of stripe deformation in magnetic-resonance tagging. IEEE Trans Med Imaging 1995;14(3):413–21.
30. Park J, Metaxas D, Young AA, et al. Deformable models with parameter functions for cardiac motion analysis from tagged MRI data. IEEE Trans Med Imaging 1996;15(3):278–89.
31. Ozturk C, McVeigh ER. Four-dimensional B-spline based motion analysis of tagged MR images: introduction and in vivo validation. Phys Med Biol 2000; 45(6):1683–702.
32. Osman NF, McVeigh ER, Prince JL. Imaging heart motion using harmonic phase MRI. IEEE Trans Med Imaging 2000;19(3):186–202.
33. Delso G, Furst S, Jakoby B, et al. Performance measurements of the Siemens mMR integrated whole-body PET/MR scanner. J Nucl Med 2011; 52(12):1914–22.
34. Wehrl HF, Sauter AW, Judenhofer MS, et al. Combined PET/MR imaging–technology and applications. Technol Cancer Res Treat 2010;9(1): 5–20.
35. Petibon Y, Ouyang J, Zhu X, et al. MR-based motion compensation in simultaneous cardiac PET-MR. J Nucl Med 2012;53(Suppl 1):108.
36. Horn BK, Schunck BG. Determining optical flow. Artif Intell 1981;17(1–3):185–203.
37. Mailloux GE, Bleau A, Bertrand M, et al. Computer-analysis of heart motion from two-dimensional echocardiograms. IEEE Trans Biomed Eng 1987; 34(5):356–64.
38. Amartur SC, Vesselle HJ. A new approach to study cardiac motion: the optical flow of cine MR images. Magn Reson Med 1993;29(1):59–67.
39. Song SM, Leahy RM. Computation of 3-D velocity fields from 3-D cine CT images of a human heart. IEEE Trans Med Imaging 1991;10(3):295–306.
40. Zhou ZY, Synolakis CE, Leahy RM, et al. Calculation of 3D internal displacement-fields from 3D X-ray computer tomographic-images. Proc R Soc London A 1995;449(1937):537–54.
41. Love AE. A treatise on the mathematical theory of elasticity. Cambridge (United Kingdom): Cambridge University Press; 1927.
42. Cao Z, Gilland DR, Mair BA, et al. Three-dimensional motion estimation with image reconstruction for gated cardiac ECT. IEEE Trans Nucl Sci 2003; 50(3):384–8.
43. Dawood M, Buther F, Jiang X, et al. Respiratory motion correction in 3-D PET data with advanced optical flow algorithms. IEEE Trans Med Imaging 2008;27(8):1164–75.
44. Beauchemin SS, Barron JL. The computation of optical flow. ACM Comput Surv 1995;27(3):433–66.
45. Barron JL, Fleet DJ, Beauchemin SS, et al. Performance of optical flow techniques. Proceedings Computer Vision and Pattern Recognition. Champaign, IL, June 15–18, 1992. p. 236–42.
46. Tang J, Segars WP, Lee TS, et al. Quantitative study of cardiac motion estimation and abnormality classification in emission computed tomography. Med Eng Phys 2011;33(5):563–72.
47. Slomka PJ, Nishina H, Berman DS, et al. "Motion-frozen" display and quantification of myocardial perfusion. J Nucl Med 2004;45(7):1128–34.
48. Brankov JG, Yang Y, Narayanan MV, et al. Motion-compensated 4D processing of gated SPECT perfusion studies. IEEE Nuclear Science Symposium Conference Record, 2002. Norfolk (VA), November 10–16, 2002. p. 1380–4.
49. Brankov JG, Yang Y, Wernick MN. Tomographic image reconstruction based on a content-adaptive mesh model. IEEE Trans Med Imaging 2004;23(2):202–12.
50. Marin T, Brankov JG. Deformable left-ventricle mesh model for motion-compensated filtering in cardiac gated SPECT. Med Phys 2010;37(10):5471–81.
51. Brankov JG, Yang Y, Wernick MN. Spatiotemporal processing of gated cardiac SPECT images using deformable mesh modeling. Med Phys 2005; 32(9):2839–49.
52. Jacobson M, Levkovitz R, Ben-Tal A, et al. Enhanced 3D PET OSEM reconstruction using inter-update Metz filtering. Phys Med Biol 2000;45(8):2417–39.
53. Mustafovic S, Thielemans K. Object dependency of resolution in reconstruction algorithms with inter-iteration filtering applied to PET data. IEEE Trans Med Imaging 2004;23(4):433–46.
54. Kadrmas DJ, Gullberg GT. 4D maximum a posteriori reconstruction in dynamic SPECT using a compartmental model-based prior. Phys Med Biol 2001;46(5):1553–74.
55. Reader AJ, Matthews JC, Sureau FC, et al. Iterative kinetic parameter estimation within fully 4D PET image reconstruction. IEEE Nuclear Science Symposium Conference Record. San Diego, CA, 29 October - 4 November, 2006. p. 1752–6.
56. Geman S, McClure DE. Statistical methods for tomographic image reconstruction. Bull Int Stat Inst 1987;52(4):5–21.
57. Chinn G, Huang SC. A general class of preconditioners for statistical iterative reconstruction of emission computed tomography. IEEE Trans Med Imaging 1997;16(1):1–10.
58. Shepp LA, Vardi Y. Maximum likelihood reconstruction for emission tomography. IEEE Trans Med Imaging 1982;1:113–22.
59. Lange K, Carson R. EM reconstruction algorithms for emission and transmission tomography. J Comput Assist Tomogr 1984;8(2):306–16.
60. Green PJ. Bayesian reconstructions from emission tomography data using a modified EM algorithm. IEEE Trans Med Imaging 1990;9:84–93.

61. Gravier EJ, Yang Y. Motion-compensated reconstruction of tomographic image sequences. IEEE Trans Nucl Sci 2005;52(1):51–6.
62. Gravier E, Yang YY, Jin MW. Tomographic reconstruction of dynamic cardiac image sequences. IEEE Trans Image Process 2007;16(4):932–42.
63. Lalush DS, Lin C, Tsui BM. A priori motion models for four-dimensional reconstruction in gated cardiac SPECT. IEEE Nuclear Science Symposium Conference Record, 1996. Anaheim (CA), November 2–9, 1996. p. 1923–7.
64. Lalush DS, Tsui BM. Block-iterative techniques for fast 4D reconstruction using a priori motion models in gated cardiac SPECT. Phys Med Biol 1998;43(4): 875–86.
65. Lee TS, Lautamaki R, Higuchi T, et al. Task-based human observer study for evaluation and optimization of 3D & 4D image reconstruction methods for gated myocardial perfusion SPECT. J Nucl Med 2009;50(Suppl 2):524.
66. Lee TS, Bengel F, Tsui BM. Task-based human observer study for evaluation of 4D MAP-RBI-EM method for gated myocardial perfusion SPECT. J Nucl Med 2008;49(Suppl 1):153P.
67. Lee TS, Segars WP, Tsui BM. Study of parameters characterizing space-time Gibbs priors for 4D MAP-RBI-EM in gated myocardial perfusion SPECT. IEEE Nuclear Science Symposium Conference Record. Wyndham El Conquistador, Puerto Rico, October 23–29, 2005. p. 2124–8.
68. Tang J, Lee TS, He X, et al. Comparison of 3D OS-EM and 4D MAP-RBI-EM reconstruction algorithms for cardiac motion abnormality classification using a motion observer. IEEE Trans Nucl Sci 2010; 57(5):2571–7.
69. Qiao F, Pan T, Clark JW Jr, et al. A motion-incorporated reconstruction method for gated PET studies. Phys Med Biol 2006;51(15):3769–83.
70. Li T, Thorndyke B, Schreibmann E, et al. Model-based image reconstruction for four-dimensional PET. Med Phys 2006;33(5):1288–98.
71. Lamare F, Cresson T, Savean J, et al. Respiratory motion correction for PET oncology applications using affine transformation of list mode data. Phys Med Biol 2007;52(1):121–40.
72. Tang J, Bengel F, Rahmim A. Cardiac motion-corrected quantitative dynamic Rb-82 PET imaging. J Nucl Med 2010;51(Suppl 2):123.
73. Hebert TJ, Leahy R. Fast methods for including attenuation in the EM algorithm. IEEE Trans Nucl Sci 1990;37(2):754–8.
74. Mumcuoglu EU, Leahy R, Cherry SR, et al. Fast gradient-based methods for Bayesian reconstruction of transmission and emission PET images. IEEE Trans Med Imaging 1994;13(4):687–701.
75. Reader AJ, Ally S, Bakatselos F, et al. One-pass list-mode EM algorithm for high-resolution 3-D PET image reconstruction into large arrays. IEEE Trans Nucl Sci 2002;49(3):693–9.
76. Daube-Witherspoon M, Yan Y, Green M, et al. Correction for motion distortion in PET by dynamic monitoring of patient position [abstract]. J Nucl Med 1990;31:816.
77. Menke M, Atkins MS, Buckley KR. Compensation methods for head motion detected during PET imaging. IEEE Trans Nucl Sci 1996;43(1):310–7.
78. Bloomfield PM, Spinks TJ, Reed J, et al. The design and implementation of a motion correction scheme for neurological PET. Phys Med Biol 2003;48(8):959–78.
79. Rahmim A, Dinelle K, Cheng JC, et al. Accurate event-driven motion compensation in high-resolution PET incorporating scattered and random events. IEEE Trans Med Imaging 2008; 27(8):1018–33.
80. Rahmim A, Bloomfield P, Houle S, et al. Motion compensation in histogram-mode and list-mode EM reconstructions: beyond the event-driven approach. IEEE Trans Nucl Sci 2004;51:2588–96.
81. Qi J, Huesman RH. List mode reconstruction for PET with motion compensation: a simulation study. Proceedings IEEE International Symposium on Biomedical Imaging, 2002. Washington, DC. July 7–10, 2002. p. 413–6.
82. Carson RE, Barker WC, Liow JS, et al. Design of a motion-compensation OSEM list-mode algorithm for resolution-recovery reconstruction for the HRRT. IEEE Nuclear Science Symposium Conference Record, 2003. Portland (OR). October 19–25, 2003. p. 3281–5.
83. Qi J. Calculation of the sensitivity image in list-mode reconstruction for PET. IEEE Trans Nucl Sci 2006;53(5):2746–51.
84. Gilland DR, Mair BA, Sun J. Joint 4D reconstruction and motion estimation in gated cardiac ECT. Proceedings of the International Meeting on Fully Three-Dimensional Image Reconstruction in Radiology and Nuclear Medicine. Salt Lake City (UT), July 6–9, 2005. p. 303–6.
85. Jacobson MW, Fessler JA. Joint estimation of image and deformation parameters in motion-corrected PET. IEEE Nuclear Science Symposium Conference Record. 2003. p. 3290–4.
86. Jacobson MW, Fessier JA. Joint estimation of respiratory motion and activity in 4D PET using CT side information. Presented at 3rd IEEE International Symposium on Biomedical Imaging: Nano to Macro. Arlington, VA, April 6–9, 2006. p. 275–8.
87. Blume M, Martinez-Moller A, Keil A, et al. Joint reconstruction of image and motion in gated positron emission tomography. IEEE Trans Med Imaging 2010;29(11):1892–906.
88. Livieratos L, Rajappan K, Stegger L, et al. Respiratory gating of cardiac PET data in list-mode

acquisition. Eur J Nucl Med Mol Imaging 2006;33(5):584–8.
89. Rahmim A, Tang J, Ay MR, et al. 4D respiratory motion-corrected Rb-82 myocardial perfusion PET imaging. IEEE Nuclear Science Symposium Conference Record. Knoxville, TN, 30 October - 6 November, 2010. p. 3312–6.
90. Park MJ, Chen S, Lee TS, et al. Generation and evaluation of a simultaneous cardiac and respiratory gated Rb-82 PET simulation. Presented at IEEE Nuclear Science Symposium and Medical Imaging Conference (NSS/MIC). Valencia, Spain, October 23–29, 2011. p. 3327–30.
91. Chen S, Bravo P, Lodge M, et al. Four-dimensional PET image reconstruction with respiratory and cardiac motion compensation from list-mode data. J Nucl Med 2012;53(1_MeetingAbstracts):106.
92. Teras M, Kokki T, Durand-Schaefer N, et al. Dual-gated cardiac PET–clinical feasibility study. Eur J Nucl Med Mol Imaging 2010;37(3):505–16.
93. Kreissl MC, Stout D, Silverman RW, et al. Heart and respiratory gating of cardiac microPET (R)/CT studies in mice. IEEE Nuclear Science Symposium Conference Record. vols. 1–7. Rome, Italy, October 19–22, 2004. p. 3877–9.
94. Klein GJ, Reutter BW, Ho MH, et al. Real-time system for respiratory-cardiac gating in positron tomography. IEEE Trans Nucl Sci 1998;45(4):2139–43.
95. Lang N, Dawood M, Büther F, et al. Organ movement reduction in PET/CT using dual-gated list-mode acquisition. Z Med Phys 2006;16(1):93–100.
96. Martinez-Möller A, Zikic D, Botnar RM, et al. Dual cardiac/respiratory gated PET: implementation and results from a feasibility study. Eur J Nuc Med Mol Imaging 2007;34(9):1447–54.
97. Yang Y, Rendig S, Siegel S, et al. Cardiac PET imaging in mice with simultaneous cardiac and respiratory gating. Phys Med Biol 2005;50(13):2979–89.
98. Schafers KP, Lang N, Stegger L, et al. Gated list-mode acquisition with the QuadHIDAC animal PET to image mouse hearts. Z Med Phys 2006;16(1):60–6.
99. Klein GJ, Reutter RW, Huesman RH. Four-dimensional affine registration models for respiratory-gated PET. IEEE Trans Nucl Sci 2001;48(3):756–60.
100. Le Meunier L, Slomka P, Fermin J, et al. Motion frozen of dual gated (cardiac and respiratory) PET images. J Nucl Med 2009;50(2_MeetingAbstracts):1474.
101. Livieratos L, Stegger L, Bloomfield PM, et al. Rigid-body transformation of list-mode projection data for respiratory motion correction in cardiac PET. Phys Med Biol 2005;14:3313–22.
102. Bruyant PP, King MA, Pretorius PH. Correction of the respiratory motion of the heart by tracking of the center of mass of thresholded projections: a simulation study using the dynamic MCAT phantom. IEEE Trans Nucl Sci 2002;49(5):2159–66.
103. Segars WP, Mori S, Chen GT, et al. Modeling respiratory motion variations in the 4D NCAT phantom. IEEE Nuclear Science Symposium Conference Record. Honolulu, Hawaii, 28 October - 3 November, 2007. NSS '07. IEEE. 2007. p. 2677–9.
104. Korin HW, Ehman RL, Riederer SJ, et al. Respiratory kinematics of the upper abdominal organs–a quantitative study. Magn Reson Med 1992;23(1):172–8.
105. Hoffman EA, Ritman EL. Heart-lung interaction: effect on regional lung air content and total heart volume. Ann Biomed Eng 1987;15(3–4):241–57.
106. Andersen K, Vik-Mo H. Effects of spontaneous respiration on left ventricular function assessed by echocardiography. Circulation 1984;69(5):874–9.
107. Qi J, Leahy RM, Chinghan H, et al. Fully 3D Bayesian image reconstruction for the ECAT EXACT HR+. IEEE Trans Nucl Sci 1998;45(3):1096–103.
108. Panin VY, Kehren F, Michel C, et al. Fully 3-D PET reconstruction with system matrix derived from point source measurements. IEEE Trans Med Imaging 2006;25(7):907–21.
109. Panin VY, Kehren F, Rothfuss H, et al. PET reconstruction with system matrix derived from point source measurements. IEEE Trans Nucl Sci 2006;53(1):152–9.
110. Alessio AM, Kinahan PE, Lewellen TK. Modeling and incorporation of system response functions in 3-D whole body PET. IEEE Trans Med Imaging 2006;25(7):828–37.
111. Rahmim A, Tang J, Lodge MA, et al. Analytic system matrix resolution modeling in PET: an application to Rb-82 cardiac imaging. Phys Med Biol 2008;53(21):5947–65.
112. Alessio AM, Stearns CW, Shan T, et al. Application and evaluation of a measured spatially variant system model for PET image reconstruction. IEEE Trans Med Imaging 2010;29(3):938–49.
113. Le Meunier L, Slomka PJ, Dey D, et al. Enhanced definition PET for cardiac imaging. J Nucl Cardiol 2010;17(3):414–26.
114. Buhler P, Just U, Will E, et al. An accurate method for correction of head movement in PET. IEEE Trans Med Imaging 2004;23(9):1176–85.
115. Tang J, Hall N, Rahmim A. MRI assisted motion correction in dual-gated 5D myocardial perfusion PET imaging. IEEE Nuclear Science Symposium Conference Record 2012, in press.
116. Bengel FM, Higuchi T, Javadi MS, et al. Cardiac positron emission tomography. J Am Coll Cardiol 2009;54(1):1–15.

117. Lodge M, Bengel F. Methodology for quantifying absolute myocardial perfusion with PET and SPECT. Curr Cardiol Rep 2007;9(2):121–8.
118. Uren NG, Melin JA, De Bruyne B, et al. Relation between myocardial blood flow and the severity of coronary-artery stenosis. N Engl J Med 1994; 330(25):1782–8.
119. Parkash R, DeKemp RA, Ruddy TD, et al. Potential utility of rubidium 82 PET quantification in patients with 3-vessel coronary artery disease. J Nucl Cardiol 2004;11(4):440–9.
120. Guethlin M, Kasel AM, Coppenrath K, et al. Delayed response of myocardial flow reserve to lipid-lowering therapy with fluvastatin. Circulation 1999;99(4):475–81.
121. Huggins GS, Pasternak RC, Alpert NM, et al. Effects of short-term treatment of hyperlipidemia on coronary vasodilator function and myocardial perfusion in regions having substantial impairment of baseline dilator reverse. Circulation 1998;98(13):1291–6.
122. Schindler TH, Nitzsche EU, Schelbert HR, et al. Positron emission tomography-measured abnormal responses of myocardial blood flow to sympathetic stimulation are associated with the risk of developing cardiovascular events. J Am Coll Cardiol 2005;45(9):1505–12.
123. Schindler TH, Nitzsche E, Magosaki N, et al. Regional myocardial perfusion defects during exercise, as assessed by three dimensional integration of morphology and function, in relation to abnormal endothelium dependent vasoreactivity of the coronary microcirculation. Heart 2003;89(5):517–26.
124. Schachinger V, Britten MB, Zeiher AM. Prognostic impact of coronary vasodilator dysfunction on adverse long-term outcome of coronary heart disease. Circulation 2000;101(16):1899–906.
125. Tsoumpas C, Turkheimer FE, Thielemans K. A survey of approaches for direct parametric image reconstruction in emission tomography. Med Phys 2008;35(9):3963–71.
126. Farncombe TH, Feng B, King MA, et al. Investigating acquisition protocols for gated, dynamic myocardial imaging in PET and SPECT. 2003 IEEE Nuclear Science Symposium Conference Record. vols. 1–5. Rome, Italy, October 19–22, 2004. p. 3272–5.
127. Feng B, Pretorius PH, Farncombe TH, et al. Simultaneous assessment of cardiac perfusion and function using 5-dimensional imaging with Tc-99m teboroxime. J Nucl Cardiol 2006;13(3):354–61.
128. Jin MW, Yang YY, King MA. Reconstruction of dynamic gated cardiac SPECT. Med Phys 2006; 33(11):4384–94.
129. Niu XF, Yang YY, Jin MW, et al. Regularized fully 5D reconstruction of cardiac gated dynamic SPECT images. IEEE Trans Nucl Sci 2010;57(3): 1085–95.
130. Niu XF, Yang YY, Wernick MN. Direct reconstruction of parametric images from cardiac gated dynamic SPECT data. Presented at 18th IEEE International Conference on Image Processing (ICIP). Brussels, Belgium, September 11–14, 2011. p. 453–6.
131. Shi YG, Karl WC. A multiphase level set method for tomographic reconstruction of dynamic objects. Proceedings of the 2003 IEEE Workshop on Statistical Signal Processing. St. Louis, Missouri, September 28 - October 1, 2003. p. 182–5.
132. Shi YG, Karl WC. Level set methods for dynamic tomography. Presented at 2nd IEEE International Symposium on Biomedical Imaging: Macro to Nano. vols. 1 and 2. Arlington, VA, April 15–18, 2004. p. 620–3.
133. Fitzpatrick GM, Wells RG. Simulation study of respiratory-induced errors in cardiac positron emission tomography/computed tomography. Med Phys 2006;33(8):2888–95.
134. Le Meunier L, Maass-Moreno R, Carrasquillo JA, et al. PET/CT imaging: effect of respiratory motion on apparent myocardial uptake. J Nucl Cardiol 2006;13(6):821–30.
135. Pan T, Mawlawi O, Nehmeh SA, et al. Attenuation correction of PET images with respiration-averaged CT images in PET/CT. J Nucl Med 2005; 46(9):1481–7.
136. Nagel CC, Bosmans G, Dekker AL, et al. Phased attenuation correction in respiration correlated computed tomography/positron emitted tomography. Med Phys 2006;33(6):1840–7.
137. Lamare F, Ledesma Carbayo MJ, Cresson T, et al. List-mode-based reconstruction for respiratory motion correction in PET using non-rigid body transformations. Phys Med Biol 2007;52(17):5187–204.
138. Bai W, Brady M. Regularized B-spline deformable registration for respiratory motion correction in PET images. Phys Med Biol 2009;54(9):2719–36.
139. Bai W, Brady M. Motion correction and attenuation correction for respiratory gated PET images. IEEE Trans Med Imaging 2011;30(2):351–65.
140. Ue H, Haneishi H, Iwanaga H, et al. Nonlinear motion correction of respiratory-gated lung SPECT images. IEEE Trans Med Imaging 2006; 25(4):486–95.
141. Fin L, Bailly P, Daouk J, et al. Motion correction based on an appropriate system matrix for statistical reconstruction of respiratory-correlated PET acquisitions. Comput Methods Programs Biomed 2009;96(3):e1–9.
142. Dawood M, Lang N, Jiang X, et al. Lung motion correction on respiratory gated 3-D PET/CT images. IEEE Trans Med Imaging 2006;25(4):476–85.
143. Liu C, Alessio AM, Kinahah PE. Respiratory motion correction for quantitative PET/CT using all detected events with internal-external motion correlation. Med Phys 2011;38(5):2715–23.

144. Chan C, Jing X, Fung EK, et al. Event-by-event respiratory motion correction for PET with 3-dimensional internal-external motion correlation, IEEE Nuclear Science Symposium Conference Record, (Anaheim, CA, 29 Oct – 3 Nov 2012), in press.
145. Lucas BD, Kanade T. An iterative image registration technique with an application to stereo vision. Presented at DARPA Image Understanding Workshop. Vancouver, British Columbia, Canada, August 24–28, 1981. p. 121–30.
146. Clifford P. Markov random fields in statistics. In: Grimmett G, Welsh DJ, editors. Disorder in physical systems. Clarendon (TX): Oxford; 1990. p. 19–32.
147. Guerin B, Cho S, Chun SY, et al. Nonrigid PET motion compensation in the lower abdomen using simultaneous tagged-MRI and PET imaging. Med Phys 2011;38(6):3025–38.
148. Chun SY, Reese TG, Ouyang J, et al. MRI-based nonrigid motion correction in simultaneous PET/MRI. J Nucl Med, in press.
149. Qiao F, Pan T, Clark JW, et al. Region of interest motion compensation for PET image reconstruction. Phys Med Biol 2007;52(10):2675–89.
150. Reyes M, Malandain G, Koulibaly PM, et al. Model-based respiratory motion compensation for emission tomography image reconstruction. Phys Med Biol 2007;52(12):3579–600.
151. Rahmim A, Cheng JC, Dinelle K, et al. System matrix modelling of externally tracked motion. Nucl Med Commun 2008;29(6):574–81.
152. Kupinski MA, Hoppin JW, Clarkson E, et al. Estimation in medical imaging without a gold standard. Acad Radiol 2002;9(3):290–7.
153. Hoppin JW, Kupinski MA, Wilson DW, et al. Evaluating estimation techniques in medical imaging without a gold standard: experimental validation. Proceedings of SPIE 2003;5034:230–7.
154. Lehmann T. From plastic to gold: a unified classification scheme for reference standards in medical image processing. Presented at Medical Imaging 2002: Image Processing. San Diego (CA), February 24–28, 2002. p. 1819–27.
155. Zaidi H, Xu XG. Computational anthropomorphic models of the human anatomy: the path to realistic Monte Carlo modeling in medical imaging. Annu Rev Biomed Eng 2007;9(1):471–500.
156. Paganetti H. Four-dimensional Monte Carlo simulation of time-dependent geometries. Phys Med Biol 2004;49(6):N75–81.
157. Segars WP, Tsui BM. MCAT to XCAT: the evolution of 4D computerized phantoms for imaging research. Proc IEEE 2009;97(12):1954–68.
158. Veress AI, Segars WP, Tsui BM, et al. Incorporation of a left ventricle finite element model defining infarction into the XCAT imaging phantom. IEEE Trans Med Imaging 2011;30(4):915–27.
159. Veress AI, Segars WP, Weiss JA, et al. Normal and pathological NCAT image and phantom data based on physiologically realistic left ventricle finite-element models. IEEE Trans Med Imaging 2006;25(12):1604–16.
160. De Bondt P, Claessens T, Rys B, et al. Accuracy of 4 different algorithms for the analysis of tomographic radionuclide ventriculography using a physical, dynamic 4-chamber cardiac phantom. J Nucl Med 2005;46(1):165–71.
161. Begemann PG, van Stevendaal U, Manzke R, et al. Evaluation of spatial and temporal resolution for ECG-gated 16-row multidetector CT using a dynamic cardiac phantom. Eur Radiol 2005;15(5):1015–26.
162. Al Hamwi A. Construction and optimal design of a dynamic heart phantom for simulation of motion artefacts in PET scan. Biomed Tech (Berl) 2002;47(Suppl 1 Pt 2):810–1 [in German].
163. Kashani R, Hub M, Kessler ML, et al. Technical note: a physical phantom for assessment of accuracy of deformable alignment algorithms. Med Phys 2007;34(7):2785–8.
164. Fitzpatrick MJ, Starkschall G, Balter P, et al. A novel platform simulating irregular motion to enhance assessment of respiration-correlated radiation therapy procedures. J Appl Clin Med Phys 2005;6(1):13–21.